Structural Insights into the ATP Binding Pocket of the Anaplastic Lymphoma Kinase by Site-Directed Mutagenesis, Inhibitor Binding Analysis, and Homology Modeling

Rosalind H. Gunby,[†,⊥] Shaheen Ahmed,[‡,⊥] Roberta Sottocornola,[†,⊥] Marc Gasser,[‡] Sara Redaelli,[†] Luca Mologni,[†] Carmen J Tartari,[†,§] Valentina Belloni,[†] Carlo Gambacorti-Passerini,*[,†,∥] and Leonardo Scapozza[‡]

Department of Clinical Medicine, Via Cadore 48, University of Milano-Bicocca, Monza, 20052, Italy, Pharmaceutical Biochemistry Group, School of Pharmaceutical Sciences, University of Geneva, University of Lausanne, Quai Ernest-Ansermet 30, CH-1211 Geneva 4, Switzerland, Department of Experimental Oncology, Istituto Nazionale dei Tumori, Via Venezian 1, Milan, 20133, Italy, and Department of Oncology, McGill University, Montreal, Canada

Received March 31, 2006

Anaplastic lymphoma kinase (ALK) is a valid target for anticancer therapy; however, potent ALK inhibitors suitable for clinical use are lacking. Because the majority of described kinase inhibitors bind in the ATP pocket of the kinase domain, we have characterized this pocket in ALK using site-directed mutagenesis, inhibition studies, and molecular modeling. Mutation of the gatekeeper residue, a key structural determinant influencing inhibitor binding, rendered the fusion protein, NPM/ALK, sensitive to inhibition by SKI-606 in the nanomolar range, while PD173955 inhibited the NPM/ALK mutant at micromolar concentrations. In contrast, both wild type and mutant NPM/ALK were insensitive to imatinib. Computer modeling indicated that docking solutions obtained with a homology model representing the intermediate conformation of the ALK kinase domain reflected closely experimental data. The good agreement between experimental and virtual results indicate that the ALK molecular models described here are useful tools for the rational design of ALK selective inhibitors. In addition, 4-phenylamino-quinoline compounds may have potential as templates for ALK inhibitors.

Introduction

The anaplastic lymphoma kinase (ALK) is a receptor tyrosine kinase normally expressed in neural tissues during embryogenesis.[1,2] As a result of chromosomal translocations involving the *alk* gene at 2p23, the ALK tyrosine kinase domain is also aberrantly expressed and constitutively activated in the form of oncogenic fusion proteins in cancers. ALK fusion proteins have been detected in anaplastic large cell lymphoma (ALCL),[3] inflammatory myofibroblastic tumors,[4] and diffuse large B cell lymphoma.[5] The most frequently occurring ALK fusion protein in ALCL is nucleophosmin (NPM)/ALK, which contains the N-terminal homodimerization domain of NPM fused to the intracellular domain of ALK, including its kinase domain.[3] Constitutive activation of the NPM/ALK kinase domain stimulates anti-apoptotic and mitogenic signaling pathways such as PI-3K/AKT, JAK/STAT, and PLCγ, resulting in cellular transformation.[6−8]

Importantly, the transforming activity of NPM/ALK is dependent on its kinase activity.[9] This fact, together with the recent demonstration that down-regulation of NPM/ALK expression using small hairpin RNA inhibits tumor growth in vivo,[10] points to ALK as a valid target for anticancer therapy. Several potential strategies for targeting ALK have been proposed, such as immunotherapy, small interfering RNAs, and inhibitors of downstream signaling pathways.[11] However, following the success of compounds such as imatinib (CGP57148B, STI571, Gleevec, Glivec),[12] the most promising approach at present is the selective and potent inhibition of ALK by small molecules that bind to the ATP pocket of the kinase domain. Nevertheless, ALK inhibitors suitable for clinical use are lacking.

Imatinib is a potent inhibitor of Abelson (Abl), stem cell factor receptor (c-Kit), platelet-derived growth factor receptor (PDGFR), and Abl-related gene (ARG).[12] It is in clinical use for the treatment of chronic myeloid leukemia (CML), gastrointestinal stromal tumors (GISTs), and hypereosinophilic syndrome (HES).[12−14] Crystal structures of the Abl kinase domain complexed with imatinib or a related derivative,[15,16] along with the crystal structures of other kinases, have allowed the characterization of conserved structural features in the ATP pocket that are important for inhibitor binding.[17] For example, the backbone of residues in the hinge region provide important hydrogen-bonding opportunities, which are exploited by the adenine ring of ATP and many potent kinase inhibitors. Indeed, imatinib forms a hydrogen bond with the backbone of the conserved methionine in Abl (M318). In addition, the hydrophobic or selectivity pocket, which flanks the ATP binding site, can be exploited to achieve inhibitor selectivity, as observed with imatinib. Because this pocket is not occupied by ATP, it is less-conserved compared with other regions of the ATP pocket. Moreover, the "gatekeeper" residue, which influences the accessibility of the selectivity pocket to small molecules, is a key determinant controlling the sensitivity of kinases to inhibitors.[18−21] The majority of kinases (75%) possess amino acids with large side chains, such as methionine (M) or phenylalanine (F), at the gatekeeper position, which limits access to the selectivity pocket. However, 25% of kinases possess small gatekeeper residues, such as threonine (T) or valine (V), that permit greater access to the selectivity pocket.[20] Indeed, mutation of the Abl gatekeeper residue (T315I) confers clinical resistance to imatinib in CML patients.[22] The conformational status of the kinase domain can also have important consequences on inhibitor binding. The three-dimensional (3D) structures of protein kinases are generally less-conserved in the inactive

* To whom correspondence should be addressed: Tel.: +39 0264488059. Fax: +39 0264488363. E-mail: carlo.gambacorti@unimib.it.
† University of Milano-Bicocca.
‡ University of Geneva.
§ Istituto Nazionale dei Tumori.
∥ McGill University.
⊥ Authors contributed equally.

10.1021/jm060380k CCC: $33.50
Published on Web 08/23/2006

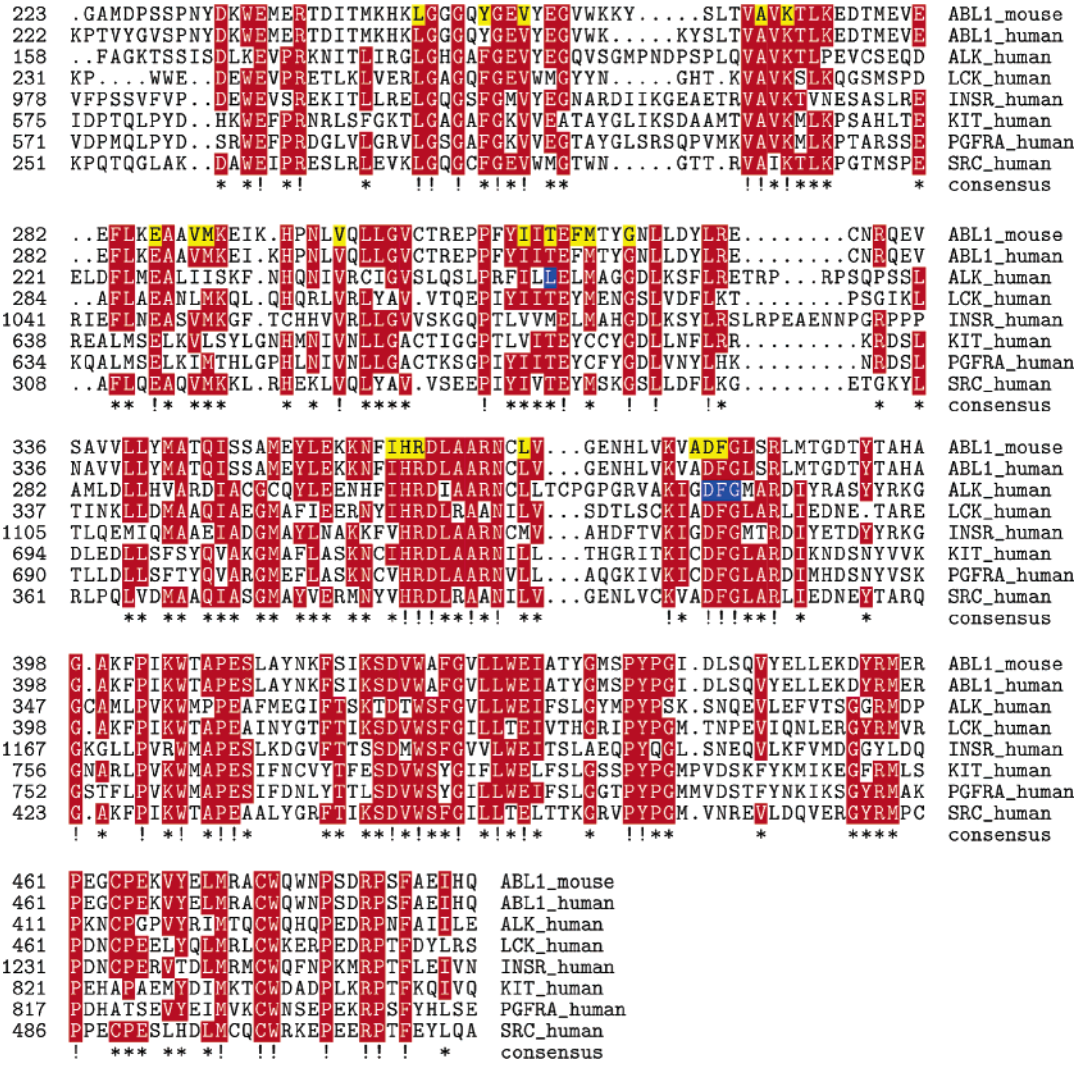

Figure 1. Multi-sequence alignment of Abl, ALK, LCK, INSR, PDGFRα, c-Kit, and Src tyrosine kinase domains. Conserved regions are shown in red. In the Abl sequence, residues that interact with imatinib, as depicted in the X-ray structure (1IEP), are highlighted in yellow. The gatekeeper residue and the conserved DFG motif in the ALK sequence are highlighted in blue. The sequence consensus is given, where "!" indicates totally conserved residues and "*" indicates a residue conservation among the majority of the aligned sequences. The kinase insert region of PDGFRα (residues 693 to 789) and c-Kit (residues 689 to 763) were removed, and the subsequent numbering of these sequences was changed accordingly. The figure was prepared using Texshade.[46]

conformation, compared with the active conformation.[23] Therefore, greater selectively may be achieved by specifically targeting the inactive conformation, as demonstrated by imatinib.

In the absence of a resolved crystal structure of ALK, we were interested in gaining structural insights into the ATP pocket of ALK. Because the gatekeeper residue and the conformational state of the kinase domain are important determinants influencing the binding of inhibitors in the ATP pocket, we investigated the impact of these determinants on inhibitor binding to ALK. We mutated the ALK gatekeeper residue and investigated both experimentally and with computer models the effect of this mutation on the sensitivity of ALK to the Abl inhibitors, imatinib, PD173955, and SKI-606. These inhibitors have been shown to form interactions with the gatekeeper residue and to bind to different conformational states of the kinase domain.[15,16,24] Computer models representing different conformational states of the ALK kinase domain were used to predict inhibitor binding modes. We observed a good agreement between experimental and modeling data, suggesting that our ALK homology models are useful tools for the rational design of ALK-specific inhibitors.

Results and Discussion

Identification of the Gatekeeper Residue in ALK by Sequence Alignment. From a multiple sequence alignment of the kinase domains of ALK, Abl, lymphocyte kinase (LCK), insulin receptor (INSR), PDGFRα, c-Kit, and Rous sarcoma protein tyrosine kinase (Src), the gatekeeper residue in ALK was identified as L1196 of ALK full length receptor (Genbank accession code: Q9UM73), equivalent to L256 of NPM/ALK (Genbank accession code: U04946) (Figure 1). Because the gatekeeper residue is one of the major determinants influencing the sensitivity of kinases to inhibitors,[20] we decided to determine the role of the ALK gatekeeper in controlling its sensitivity to imatinib, PD173955, and SKI-606 (Figure 2). The crystal structures of Abl complexed with imatinib and PD173955 have shown that these inhibitors interact directly with the gatekeeper residue of Abl, T315, forming a hydrogen bond or van der Waals interactions, respectively.[15,16] In addition, these inhibitors are unable to effectively inhibit the T315I Bcr/Abl mutant[22,25] (Gambacorti-Passerini, C., unpublished results), highlighting the importance of the gatekeeper residue in the binding of these compounds to the ATP pocket. Therefore, it was hypothesized

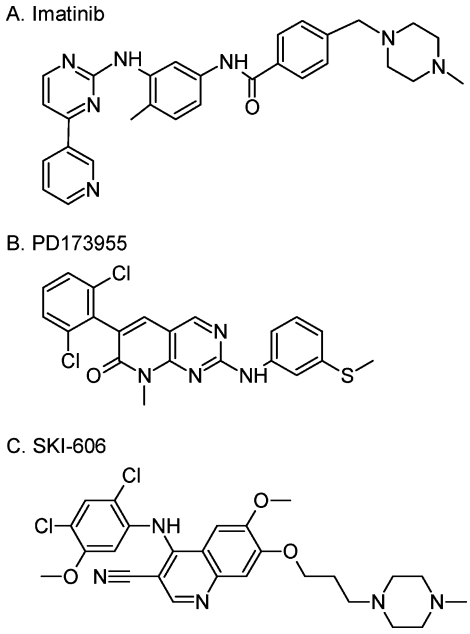

Figure 2. Chemical structures of imatinib (A), PD173955 (B), and SKI-606 (C).

that replacement of L256 with T in NPM/ALK should favor the binding of these inhibitors and result in the inhibition of NPM/ALK kinase activity.

Mutation of the Gatekeeper Renders NPM/ALK Sensitive to the Inhibitors PD173955 and SKI-606, but not Imatinib. BaF3 cell lines stably transfected with wild-type (WT) or L256T mutant NPM/ALK were generated and treated with inhibitors. Because the gatekeeper residue does not contact directly ATP, its substitution should not have a major impact on catalytic activity.[15,22] Indeed, the L256T mutation did not appear to influence the overall kinase activity, as autophosphorylation activity of L256T-NPM/ALK was comparable to that of WT-NPM/ALK (data not shown). Moreover, L256T-NPM/ALK induced IL-3 independent growth in BaF3 cells in a fashion similar to WT-NPM/ALK.

The sensitivities of WT- and L256T-NPM/ALK to the inhibitors imatinib, PD173955, and SKI-606 were assessed. As expected, WT-NPM/ALK was insensitive to all of the inhibitors, even at high micromolar concentrations (Figures 3 and 4). In contrast, the autophosphorylation activity of L256T-NPM/ALK was inhibited by both PD173955 and SKI-606, but not imatinib, as assessed by antiphosphotyrosine immunoblotting of whole cell lysates (Figure 3) and confirmed in an in vitro radioactive kinase assay (Figure 4). SKI-606 was the most potent inhibitor of L256T-NPM/ALK, with an IC_{50} value of approximately 150 nM, similar to its IC_{50} on Bcr/Abl, determined in comparable assays (from 25 to 50 nM).[26] In contrast, PD173955 was a less-potent inhibitor of L256T-NPM/ALK, with an IC_{50} of approximately 2.5 μM. In comparison, PD173955 has been reported to inhibit Bcr/Abl in similar assays, with an IC_{50} of 2−10 nM.[27] This difference in IC_{50} values suggests that the ATP binding pocket of L256T-NPM/ALK accommodates SKI-606 better than PD173955.

Consistent with the ability of SKI-606 to inhibit L256T-NPM/ALK autophosphorylation, SKI-606 also selectively inhibited cell proliferation in BaF3 cells transformed with L256T-NPM/ALK, compared with cells transformed with WT-NPM/ALK or transfected with empty vector (EV) alone (Figure 5A). BaF3-L256T cells were approximately five times more sensitive to SKI-606 than BaF3−WT and BaF3-EV cells, with IC_{50} values

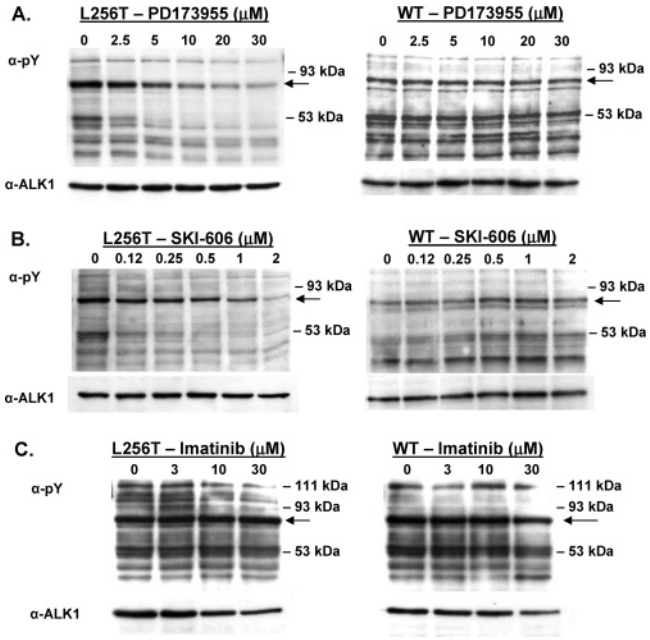

Figure 3. PD173955 and SKI-606 inhibit L256T-NPM/ALK, but not WT-NPM/ALK autophosphorylation in cells. Antiphosphotyrosine (α-pY) and anti-ALK (α-ALK1) immunoblotting of BaF3-L256T and BaF3-WT cells treated for 2 h with the indicated concentrations of PD173955 (A), SKI-606 (B), or imatinib (C). Control samples were treated with an equivalent volume of solvent alone. Arrows indicate tyrosine phosphorylated NPM/ALK.

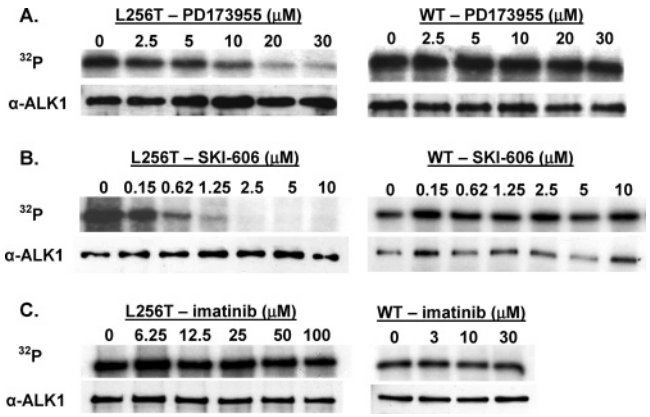

Figure 4. PD173955 and SKI-606 inhibit autophosphorylation of immunoprecipitated L256T-NPM/ALK, but not WT-NPM/ALK. Autoradiographs of in vitro radioactive kinase assays, where immunoprecipitated L256T- and WT-NPM/ALK autophosphorylation was stimulated in the presence of the indicated concentrations of PD173955 (A), SKI-606 (B), or imatinib (C). Control samples were treated with equivalent volumes of vehicle. Protein loading was controlled by anti-ALK immunoblotting.

of 0.2 ± 0.02 μM versus 1.0 ± 0.07 μM and 1.1 ± 0.09 μM, respectively (mean ± s.e.m.; significance $p < 0.0001$). In contrast, both PD173955 and imatinib showed nonspecific toxicity against all BaF3 transfectants (Table 1). The inability of PD173955 to selectively inhibit BaF3-L256T cell proliferation, despite its activity against L256T-NPM/ALK, likely reflects the relatively low potency of this compound on the NPM/ALK mutant and its lack of selectivity at micromolar concentrations. However, both SKI-606 and PD173955 selectively induced cell death in BaF3-L256T cells assessed by trypan blue exclusion. SKI-606 induced a 7-fold increase in cell death in BaF3-L256T samples compared with those of BaF3-WT and BaF3-EV samples, respectively, while PD173955, after a limited incuba-

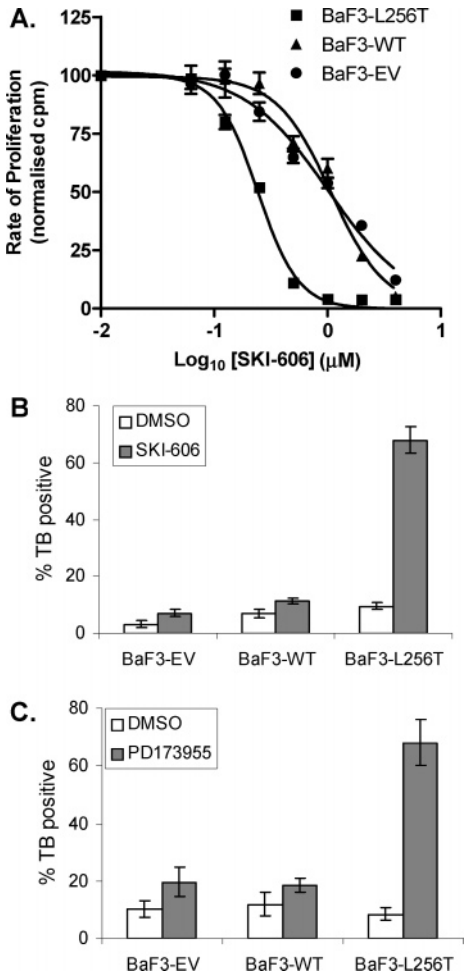

Figure 5. SKI-606 and PD173955 selectively inhibit proliferation and induce cell death in BaF3 cells transformed with L256T-NPM/ALK. (A) Proliferation was measured by tritiated thymidine uptake in BaF3-L256T, -WT, and -EV cells treated with 0−4 μM SKI-606 for 48 h. Results were normalized against vehicle control. (B) Cells were treated with 1 μM SKI-606 for 48 h or (C) 10 μM PD173955 for 16 h, and cell death was determined by trypan blue (TB) staining. Control samples were treated with vehicle alone (DMSO). Over 200 cells were counted for each sample. Results are representative of three repeats.

tion time of 16 h, induced a 3.5-fold increase in cell death (Figure 5B,C). Longer incubations with PD173955 resulted in nonspecific cell death in all cell lines.

Therefore, substitution of the gatekeeper residue was sufficient to allow inhibition of NPM/ALK by SKI-606 and PD173955, pointing to the critical role of the gatekeeper residue in binding these inhibitors. In contrast, mutant NPM/ALK was not sensitive to imatinib, suggesting that structural features other than the gatekeeper residue are preventing imatinib from binding. Interestingly, from the alignment of the ALK and Abl kinase domain sequences, it was observed that ALK differs from Abl at 13 amino acids that are mutated in imatinib-resistant CML patients. Moreover, at three of these positions, the amino acid in ALK is identical to that observed in the mutated Bcr/Abl (Y253F, F317L, and V379I; Figure 1). These differences in amino acid sequence may be responsible for the inactivity of imatinib on L256T-NPM/ALK. This hypothesis is supported by the finding that SKI-606 and PD173955 inhibit L256T-NPM/ALK, as these compounds are able to inhibit many imatinib-resistant Bcr/Abl mutants, such as H369P, Y253H, and E255K[25] (Gambacorti-Passerini, C., unpublished results). In addition to amino acid differences, the conformational status of the ALK kinase domain may affect imatinib binding. Because imatinib has a strict preference for the closed/inactive conformation of Abl, while PD173955 and probably SKI-606 bind to intermediate conformations of Abl,[16,24] it is possible that a very closed, inactive conformation of ALK is not favored, hence, preventing imatinib from binding. To gain a more detailed insight into the structural determinants influencing the binding of inhibitors to ALK, computer modeling was performed.

Generation of Computer Models of the ALK Kinase Domain. Because the conformational status of the kinase domain can have important consequences on inhibitor binding,[28] 3D homology models representing the inactive, intermediate, and active conformations of the WT- and L256T-ALK kinase domains were generated. The structures of kinases with inactive/closed (mouse c-Abl and mouse INSR, PDB codes: 1IEP, 1OPJ, and 1IRK[15,16,29]), intermediate (c-mouse Abl, 1M52[16]), and active/open conformations (mouse INSR and human LCK, 1IR3, and 3LCK[30,31]) were used as templates. The overall ALK structures with highlighted activation loops and DFG motifs are shown (Figure 6). The inactive/closed conformation of a tyrosine kinase is defined by a closed activation loop and an orientation of the DFG motif that results in the phenylalanine pointing toward the nucleotide binding pocket, thereby preventing ATP from binding. In the active/open conformation, the activation loop is open and the aspartate of the DFG motif points toward the nucleotide binding pocket, contributing to the binding of ATP. Finally, in the intermediate conformation the activation loop is in an open conformation as seen in active tyrosine kinases, however, the DFG motif is in a nonproductive conformation similar to that observed in inactive tyrosine kinases.

Docking Analyses. To validate our docking procedure, PD173955 and imatinib were first redocked into their corresponding crystal structure of Abl,[15,16] and binding modes were compared with those observed by crystallography. The best docking solutions were achieved using FlexX,[32] which faithfully reproduced the binding modes of PD173955 and imatinib in their X-ray structures, with root-mean-square deviation (RMSD) values of 0.7 and 0.6 Å, respectively (Figure 7A). FlexX was subsequently used to dock SKI-606, PD173955, and imatinib in the different conformational models of the WT and L256T ALK kinase domain.

SKI-606. The docking of SKI-606 in the inactive, intermediate, and active models of ALK-WT revealed a binding mode of SKI-606 on the surface of the kinase domain, outside the catalytic site, in all three models, as shown in a representative manner in Figure 7B (left panel). From this binding mode, SKI-606 would not be expected to inhibit ALK-WT, which is in agreement with experimental data (Table 1). In contrast, for the ALK-L256T models, docking solutions inside the ATP pocket were obtained with the intermediate and active conformations, while for the inactive conformation, SKI-606 was docked outside the ATP binding pocket.

In the ALK-L256T intermediate model, SKI-606 formed two hydrogen bonds with the catalytic site: one between its cyano group and the −OH of the mutated T256 gatekeeper residue and the other between the nitrogen of its quinoline moiety and the backbone of a conserved methionine (M259) of the hinge region (Figure 7B, middle panel; Figure 8A). In addition, the 2,4-dichlorine-5-methoxy-phenyl moiety of SKI-606 that occupies a volume of 120.8 Å^3 inserts in the selectivity pocket forming strong apolar interactions, while the piperazine moiety is orientated toward the solvent (Figure 8A). Interestingly, this binding mode of SKI-606 is very similar to the recently

Table 1. Summary of IC_{50} Values Obtained for Imatinib, SKI-606, and PD173955 for WT and L256T NPM/ALK

	IC_{50} values N/A-WT (μM)			IC_{50} values N/A-L256T (μM)		
assay	imatinib	SKI-606	PD173955	imatinib	SKI-606	PD173955
immunoblotting	>30	>20	>30	>30	0.2	3
kinase assay	>30	>10	>30	>100	0.15	2.5
proliferation[a]	7.1 ± 1.0	1.0 ± 0.07	2.0 ± 0.3	9.1 ± 1.1	0.2 ± 0.02	1.8 ± 0.1

[a] IC_{50} values are expressed as the mean ± s.e.m. of three or more independent repeats.

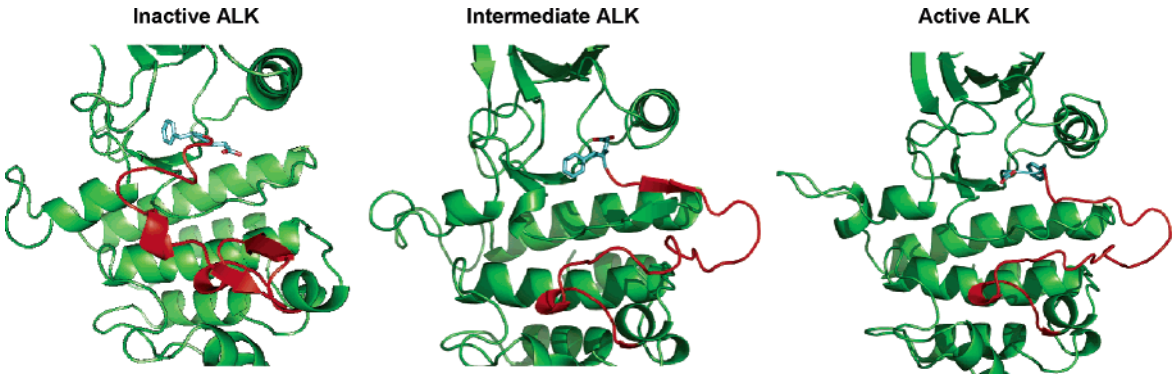

Figure 6. ALK models of the inactive, intermediate, and active conformation. The activation loop is colored in red, and the phenylalanine and aspartate of the DFG motif are shown in color-coded sticks (O, red; C, gray/blue).

described binding mode of SKI-like compounds docked into Src and Abl.[24]

In the ALK-L256T active model, the binding mode of SKI-606 differs from that observed in the intermediate conformation: the cyano group of SKI-606 forms a hydrogen bond with the hinge region (M259) instead of the gatekeeper, replacing the quinoline interaction with the hinge region seen in the intermediate model (Figure 7B, right panel, Figure 8C). A second hydrogen bond is formed between the amino group linking the 2,4-dichlorine-5-methoxy-phenyl and the quinoline and the −OH of the T256 gatekeeper residue (Figure 8C). The 2,4-dichlorine-5-methoxy-phenyl moiety remains inserted partially in the selectivity pocket, and the piperazine moiety is orientated toward the solvent in an orthogonal manner, compared to the binding mode in the intermediate conformation (Figure 7B). In this orientation, the quinoline moiety and the hydrogen bond formed by the cyano group with the M259 remain solvent exposed, and their contribution in terms of binding is lower. Thus, this binding mode seems to be less-favorable compared to the one described within the intermediate conformation.

The binding modes observed for SKI-606 in the ALK-L256T models suggest that SKI-606 forms strong interactions with the ALK-L256T catalytic site, supporting our experimental findings showing that SKI-606 is a potent inhibitor of L256T-NPM/ALK (Table 1). Taking together experimental and modeling data, it can be concluded that the gatekeeper residue plays a decisive role in SKI-606 binding and that the structural characteristics of the ATP binding pocket of ALK in the intermediate and active conformations, excluding the gatekeeper residue, are permissive to SKI-606 binding.

PD173955. For PD173955, all docking solutions in the active and inactive conformations of ALK-WT were located on the surface of the kinase domain (data not shown). In comparison, docking of PD173955 in the ALK-WT intermediate conformation led to two distinct docking poses. In two-thirds of cases, a binding mode similar (RMSD = 0.9 Å) to that in the Abl crystal structure 1M52 (Figure 7A, left panel) was observed (Figure 7C, left panels: rose). In the remaining one-third of cases, the orientation of PD173955 was inverted by 180° (head and tail position switched) and shifted toward the solvent with respect to the binding mode observed in the 1M52 crystal structure (Figure 7C, left panel: cyan).

For the ALK-L256T models, PD173955 was docked in the ATP pocket in the intermediate and active conformations, but not the inactive conformation, where PD173955 docked outside of the ATP binding pocket. Docking of PD173955 in the ALK-L256T intermediate conformation model yielded a single binding mode (Figure 7C, middle panel, Figure 8B), almost identical (RMSD = 0.8 Å) to the binding mode observed in the 1M52 crystal structure of Abl (Figure 7A, left panel). In contrast, docking of PD173955 in the ALK-L256T active conformation model led to a binding mode that was flipped 180° along the molecule axis with respect to its conformation in the crystal structure of 1M52 (Figure 7C, right panel). In this binding mode, PD173955 exhibits only weak interactions with the hinge region and, more importantly, does not occupy the selectivity pocket with its 1,5-dichlorine-phenyl moiety, suggesting a rather weak binding to this conformation of ALK-L256T (Figure 8D).

The different docking solutions obtained with ALK-L256T and ALK-WT intermediate models, point to a key role of the gatekeeper residue in orientating PD173955 correctly in the ATP pocket. The alternative binding modes of PD173955 in intermediate ALK-WT model (Figure 7C, left panel) suggest a weaker interaction between inhibitor and kinase compared with the ALK-L256T intermediate conformation model for which only one binding solution was observed. Therefore, based on this docking analysis, PD173955 was expected to be a better inhibitor of mutated NPM/ALK than WT. Indeed, experimental data showed that PD173955 inhibited L256T-NPM/ALK, but not WT-NPM/ALK at concentrations up to 30 μM (Table 1). However, it cannot be excluded that at higher concentrations PD173955 would also inhibit WT-NPM/ALK. Owing to the poor solubility of this compound, higher concentrations could not be tested.

Despite the almost identical binding modes of PD173955 in the ALK-L256T intermediate homology model and the Abl 1M52 crystal structure, PD173955 is a much more potent inhibitor of Bcr/Abl compared with L256T-NPM/ALK. This difference in potency may be explained by variations in the

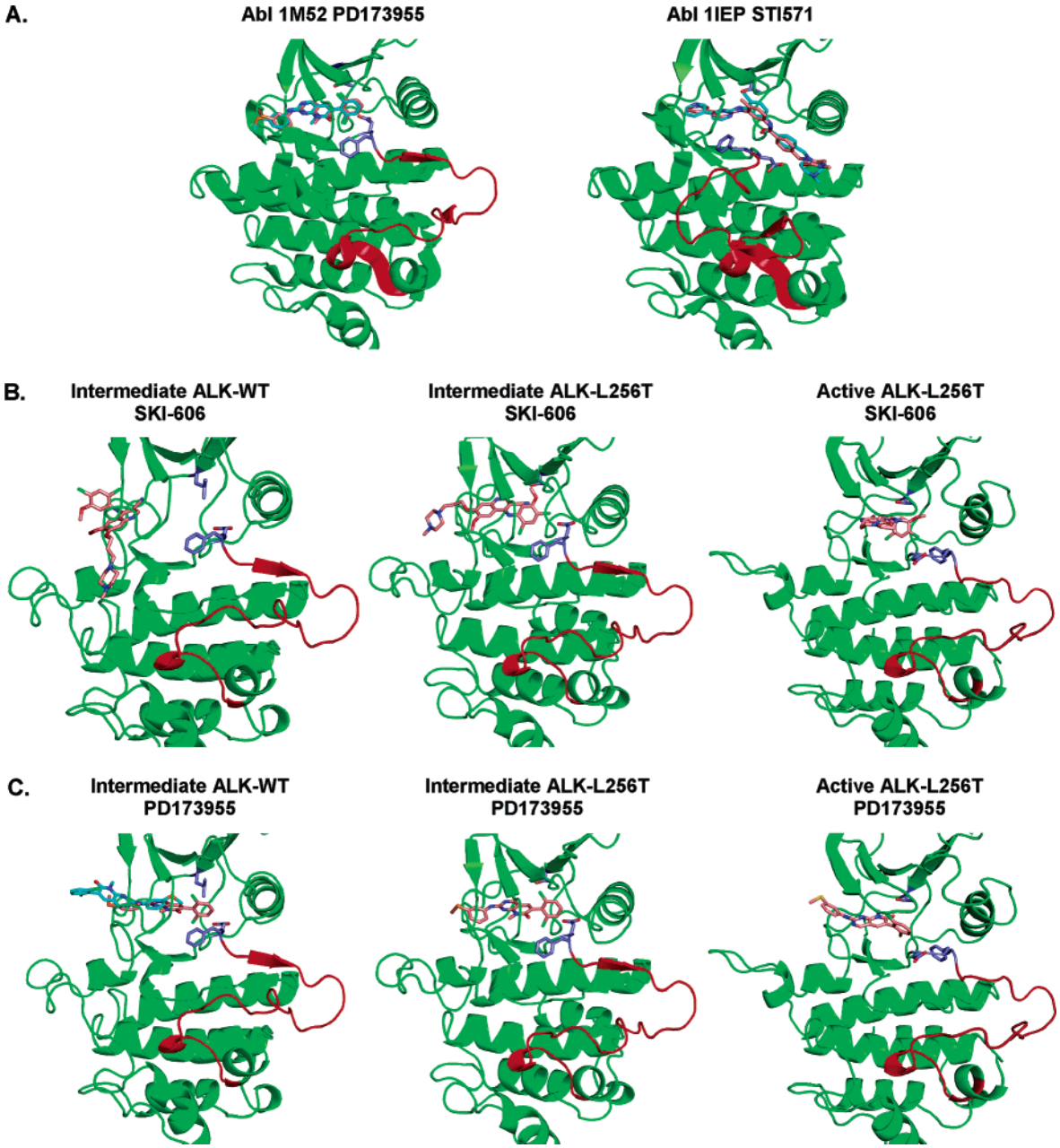

Figure 7. Docking of inhibitors in ALK models. (A) Validation of the docking protocol. Docking of PD173955 and imatinib into Abl, 1M52, and 1IEP, respectively. PD173955 and imatinib are shown in color-coded sticks (O, red; N, blue; Cl, green; S, orange). The carbon atoms of the docked solution are colored in pink and those of the crystal structure are colored in cyan. Docking of SKI-606 (B) and PD173955 (C) in the intermediate conformation of ALK-WT (left panel) and the intermediate (middle panel) and active (right panel) conformations of ALK-L256T. Inhibitors are shown in color-coded sticks, as described in part (A) with pink carbon atoms. In panel C left, the predominant binding mode of PD173955 in ALK-WT is shown with pink carbons, while the alternative binding mode is shown with cyan carbons. The activation loop is colored in red. The DFG motif and the gatekeeper residue are shown in color-coded sticks (O, red; C, purple).

amino acid composition of the ATP pockets of the two kinases and the stringent binding mode of PD173955. Modeling studies revealed that the positioning of PD173955 in the catalytic sites of both ALK-L256T and Abl is driven by strong interactions with the backbone of the conserved methionine (M259 in NPM/ALK; M318 in Abl) in the hinge region (Figure 8B). These strong interactions lead to an inflexible binding mode, reducing the capacity of PD173955 to compensate for unfavorable interactions with the protein near the gatekeeper residue. Therefore, amino acid differences between the ATP pockets of ALK and Abl are likely to have a marked impact on the binding affinity of PD173955, as reflected by IC_{50} values.

The finding that SKI-606 is a more potent inhibitor of L256T-NPM/ALK compared with PD173955 can be explained by several observations. SKI-606, but not PD173955, forms an electrostatic interaction with the −OH of the mutated gatekeeper residue (Figure 8A,B). In addition, from visual inspection of binding modes, the 1,4-dichlorine-5-methoxy of SKI-606, occupying a volume of 120.8 $Å^3$, fills the selectivity pocket much better than the corresponding 1,5-dichloro-phenyl moiety of PD173955 that occupies a volume of 97.9 $Å^3$, thus leading to more favorable hydrophobic interactions. Finally, SKI-606 is conformationally less-restricted than PD173955 due to a different hydrogen bond pattern at the hinge region (one hydrogen bond instead of two; Figure 8).

The fact that both PD173955 and SKI-606 have different binding modes in the active conformation of ALK-L256T compared with that of the intermediate conformation (Figure

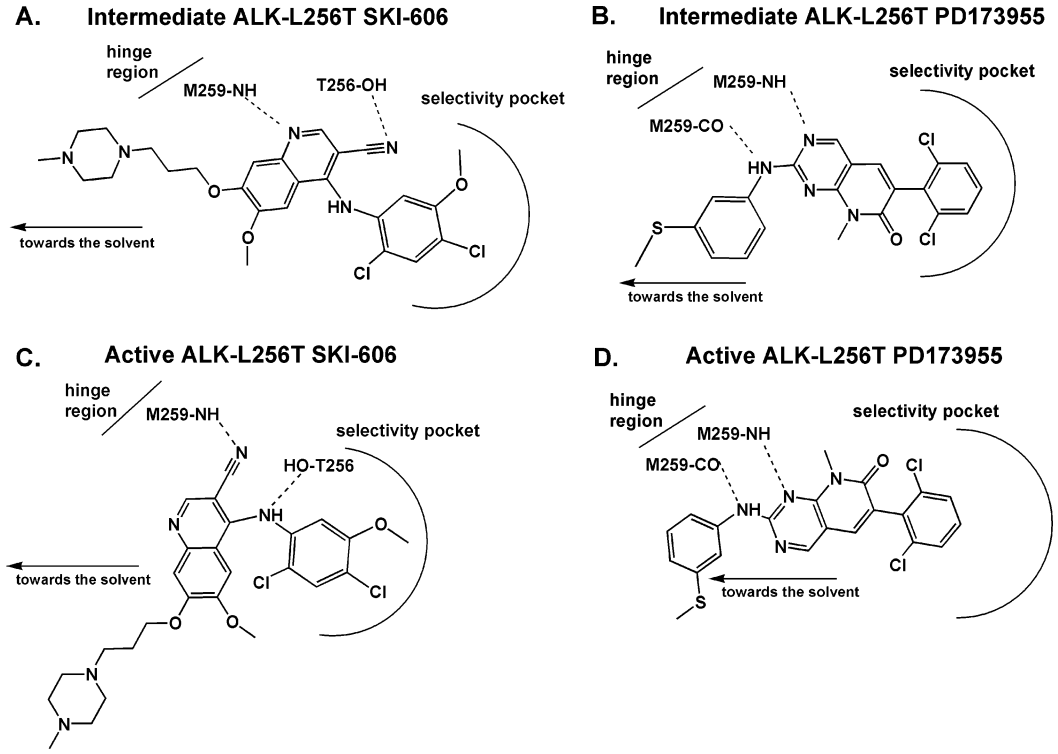

Figure 8. Schematic diagram of the interactions made by SKI-606 and PD173955 docked in the 3D model of the intermediate (A, SKI-606; B, PD173955) and active (C, SKI-606; D, PD173955) conformations of the L256T-ALK kinase domain. Amino acid residues forming hydrogen bonds (dotted lines) are shown. The selectivity pocket and the hinge region are indicated by a semicircled and a straight line, respectively. Residues forming the selectivity pocket are: I231, V240, C242, I254, T256 (mutated gatekeeper), and G329. Residues forming the hinge region are: E257, L258, M259, A260, G261, G262, and D263.

7B,C, middle and right panels) can be explained by alterations in the conformation of the DFG motif (Figure 6, middle and right panel). In the intermediate model, the relatively bulky hydrophobic side chain of Phe is pointing toward the nucleotide binding site, while in the active conformation, the smaller polar side chain of Asp is pointing inward. These different orientations of the phenylalanine and aspartate of the DFG motif not only introduce different steric constraints in the catalytic site, but more importantly change its physicochemical features. These changes render the catalytic site of the active conformation much more polar in the region where the hydrophobic moiety of the inhibitor is placed in the intermediate conformation. With PD173955, these changes cause a 180° flip along the molecule axis, resulting in a binding mode where the 1,5-dichlorine-phenyl hydrophobic moiety no longer targets the selectivity pocket (Figure 8D). However, for SKI-606, the presence of the amino moiety as a linker between the 2,4-dichlorine-5-methoxy-phenyl moiety and the quinoline (Figure 2) allows the substituted phenyl to fill the selectivity pocket in the ALK-L256T active model (Figure 8C). Therefore, the orientation of the DFG motif has a marked impact on the placement of ligands targeting this region.[21]

Imatinib. The docking of imatinib in the inactive and intermediate conformations of both the ALK-WT and the ALK-L256T models resulted in a binding mode outside the ATP binding pocket (data not shown). The binding mode observed in the inactive conformation of Abl in the 1IEP crystal structure (Figure 7A, right panel)[15] was not reproduced in any of the ALK models, including the inactive conformation of the L256T mutant. Therefore, unlike PD173955 and SKI-606, substitution of the bulky gatekeeper residue in ALK with a smaller residue was not sufficient to allow imatinib to bind, indicating that other structural determinants prevent imatinib from binding. Similarly, mutation of gatekeeper in the INSR and fibroblast growth factor receptor (FGFR) did not render these kinases sensitive to imatinib.[21] In contrast, mutation of the FLT-3 gatekeeper, F691, to T converted this kinase into a target of imatinib.[21] Modeling analysis of the INSR revealed that in its inactive conformation the DFG motif is configured in such a way as to clash with imatinib.[21] However, superimposing the imatinib conformation taken from 1IEP onto the ALK inactive model does not result in a clash with the DFG motif and, therefore, cannot explain the lack of binding to the ALK inactive model. Because imatinib binding is conformationally very demanding, small changes in the conformation of residues in the catalytic site may be sufficient to prevent its binding. In addition, as imatinib enters more deeply into the selectivity pocket behind the gatekeeper residue than PD173955 and SKI-606,[16] it is reasonable to assume that differences in the amino acid composition of this pocket and of other regions in the active site of the ALK-L256T inactive model, compared to Abl inactive, prevent imatinib binding. From the 19 residues reported by Nagar et al. to interact with imatinib, six are altered in NPM/ALK. These are Y253F (nucleotide binding loop), V289I, M290I (α-helix C), T315L (gatekeeper), F317L (hinge region), and A380G (residue preceding the DFG motif; Figure 1).

In the active conformation of ALK-WT and ALK-L256T, docking solutions inside the ATP pocket were obtained (Figure S1). Interestingly, imatinib was docked in the active ALK models with a compact *cis*-conformation, very similar to the conformation observed in the resolved crystal structure of the spleen tyrosine kinase (SYK) complexed with imatinib (PDB code: XBB).[33] In this *cis*-conformation, imatinib still interacts with the hinge region, but no longer interacts with the selectivity pocket nor the gatekeeper residue, as seen in the *trans*-conformation in the 1IEP crystal structure. Because a weaker

Table 2. Summary of the Docking Modes of SKI-606, PD173955, and Imatinib in the ALK-WT and ALK-L256T Homology Models[a]

	ALK-WT			ALK-L256T		
inhibitor	inactive	intermediate	active	inactive	intermediate	active
SKI-606	−	−	−	−	+[d]	+[d]
PD173955	−	+[b]	−	−	+[d]	+[d]
imatinib	−	−	+[c]	−	−	+[c]

[a] The symbol "−" indicates that the compound docked on the surface of the kinase domain and not in the ATP pocket, and the symbol "+" indicates a binding mode inside the ATP pocket. [b] Two binding modes (Figure 7C). [c] *cis*-Conformation. [d] See Figure 8.

binding of imatinib in this *cis*-conformation has been observed for SYK,[33] imatinib would not be expected to inhibit ALK at micromolar concentrations, in line with experimental findings.

Conclusions

ALK fusion proteins are valid molecular targets for anticancer drugs.[10] However, to date, few ALK inhibitors have been described and no molecules suitable for clinical use have been developed. Two fused pyrrolocarbazoles, CEP-14083 and CEP-14513, have recently been reported to inhibit ALK (IC_{50} < 30 nM) with reasonable selectivity.[34] However, these compounds are not suitable for use in vivo due to unfavorable physical properties. In addition, 5-aryl-pyridone carboxamides have been reported as ALK inhibitors, although specificity and potency of these compounds in cellular assays are so far poor.[35]

In the absence of a resolved structure of ALK, 3D models are valuable starting points for generating ideas for the drug-development process. We have generated homology models of the ALK kinase domain in different conformational states and used them to rationalize experimental findings relating to the sensitivity of WT-ALK and the gatekeeper mutant L256T-ALK to various inhibitors (summarized in Tables 1 and 2). We observed that mutation of the bulky leucine gatekeeper residue in ALK to a smaller threonine residue was sufficient to allow binding of the inhibitors SKI-606 and PD173955 inside the ATP pocket and, consequently, inhibition of mutated ALK. Hence, the gatekeeper residue is an important anchor point for the compounds, guiding their correct orientation in L256T-ALK. Docking solutions for SKI-606 and PD173955 were obtained with the intermediate and active conformations of L256T-ALK, but not the inactive conformation. However, binding modes in the intermediate conformation correlated better with the observed potency of these compounds experimentally, as the inhibitors displayed stronger and more numerous interactions with the ATP pocket in this conformation compared with the active conformation. However, it cannot be excluded that inhibitors are binding to both the intermediate and active conformations. The different binding modes in the active and intermediate conformations likely reflects the different orientations of the DFG motif, which in the active conformation renders the ATP pocket much more polar, hindering the binding of the hydrophobic moiety of the inhibitors. The observation that SKI-606 was a relatively potent inhibitor of L256T-NPM/ALK suggests that 4-phenylamino-quinoline compounds have potential as templates for ALK inhibitors. In line with this idea, two 4-phenylamino-quinazoline compounds, WHI-P131 and WHI-P154, have recently been described to inhibit NPM/ALK, albeit with IC_{50} values in the micromolar range (5−10 μM).[36] For imatinib, structural determinants in addition to the gatekeeper residue prevent it from binding. In conclusion, the 3D molecular models described here are useful tools for the rational design of ALK inhibitors. The data also highlight the importance of considering different conformational states of the kinase domain when performing virtual screens for potential new inhibitors.

Experimental Procedures

Mutagenesis and Cell Culture. Full length human NPM/ALK cDNA, subcloned in the expression vector pcDNA3.0, was kindly provided by Dr. P. G. Pelicci (European Institute of Oncology, Milan). Point mutations were introduced using the QuickChangeXL site-directed mutagenesis kit (Stratagene), according to manufacturer's instructions and verified by DNA sequencing. IL-3-dependent murine pro-B cells, BaF3 (5×10^6), were transfected with 10 μg pcDNA3 containing WT NPM/ALK, L256T mutant NPM/ALK, or the EV by electroporation. Transfected cells were selected by culturing in the presence of G418 (0.8 mg/mL) for 2 weeks. WT- or L256T-NPM/ALK transformed cells were further selected by withdrawing IL-3. Single cell clones were obtained by limiting dilution in 96-well plates, and expression of the correct construct was verified by RT-PCR and DNA sequencing. NPM/ALK expression was also verified by immunoblotting. Cells were maintained in RPMI 1640 media (BioWhittaker), supplemented with 10% FBS, 2 mM L-glutamine, 100 U/ml penicillin G, 80 μg/mL gentamycin, 20 mM HEPES. Control cells transfected with pcDNA3.0 alone were cultured in the presence of 0.2% supernatant from CHO cells expressing IL-3. All cells were cultured in a humidified atmosphere at 37 °C and 5% CO_2.

Inhibition Studies. The pyrido-[2,3-*d*]pyrimidine inhibitor, PD173955, was kindly supplied by Pfizer (Groton, CT). The 4-anilino-3-quinolinecarbonitrile, SKI-606, was kindly provided by Wyeth Research (Pearl River, NY).[37] Both inhibitors were dissolved in DMSO and stored at −20 °C. The 2-phenylaminopyrimidine derivative, imatinib, was supplied by Norvatis, Inc. (Basel, Switzerland), and prepared as described previously.[38]

The effect of inhibitors on tyrosine phosphorylation levels of NPM/ALK in cells was assessed by immunoblotting. Cells (2×10^6) were treated for 2 h with the indicated concentrations of inhibitors or vehicle alone. Cells were washed in ice cold PBS and lysed on ice for 30 min in lysis buffer (25 mM Tris-HCl pH 7.4, 150 mM NaCl, 1% Triton X-100, 5 mM EDTA, 5 mM EGTA, 1 mM $NaVO_4$, 1 mM DTT, 1 mM PMSF, and 10 μg/mL of pepstatin A, leupeptin, and aprotinin). Lysates were subjected to SDS-PAGE and western blotting. Tyrosine phosphorylated proteins were detected using the mouse monoclonal antiphosphotyrosine 4G10 antibody (Upstate Biotechnology). NPM/ALK was detected using a monoclonal anti-ALK1 antibody provided by Dr. K. Pulford (Nuffield Department of Clinical Laboratory Sciences, John Radcliffe Hospital, Oxford, U.K.). IC_{50} values were estimated semiquantitatively by densitometry.

The effect of inhibitors on NPM/ALK kinase activity was assessed in vitro by a radioenzymatic assay. WT- or L256T-NPM/ALK proteins were immunoprecipitated from 20×10^6 cells using the monoclonal anti-ALK1 antibody and Gammabind G Sepharose beads (Amersham Pharmacia Biotech). Immunocomplexes were washed five times in lysis buffer, once in kinase buffer (25 mM Hepes pH 7.0, 5 mM $MgCl_2$, and 5 mM $MnCl_2$), and then preincubated with inhibitors at indicated concentrations for 15 min at room temperature. NPM/ALK autophosphorylation was stimulated by incubating immunocomplexes at 30 °C for 20 min in the presence of reaction buffer (kinase buffer plus 1 mM DTT, 30 μM cold ATP, and 10 μCi [γ^{32}]P-ATP). The reaction was stopped by adding SDS-gel loading buffer and heating samples at 95 °C for 10 min. Proteins were subjected to SDS-PAGE and western blotting. Incorporation of [γ^{32}]P-ATP was visualized by autoradiography, and IC_{50} values were estimated semiquantitatively by densitometry.

The effect of inhibitors on cell proliferation and viability was assessed by ^{3}[H]-thymidine uptake and trypan blue exclusion, respectively, as described previously.[38] Briefly, in proliferation, assays cells were seeded in a 96-well plate (10^4/well) and treated with inhibitors or vehicle alone for 8−48 h. The IC_{50} was defined as the concentration that resulted in a 50% decrease in ^{3}[H]-thymidine uptake, compared with that of controls, and was

calculated using GraphPad Prism software. In viability assays, cells (2×10^6) were treated with 10 μM PD173955 or 1 μM SKI-606 for 16 or 48 h, respectively. Control samples received an equivalent volume of DMSO alone.

Generation of the ALK 3D Molecular Models. Three models of ALK corresponding to a closed, intermediate, and open conformation of the catalytic site were generated using the following protocol. The sequences of human ALK and Abl were retrieved from the SwissProt database[39] (accession codes Q9UM73 and P00519, respectively), and the kinase domain sequence was extracted. The tyrosine kinase sequence of human ALK, spanning over 278 residues, was taken as a query to search the pdb database using PSI-Blast[40] to find putative templates for ALK homology modeling. Further filtering criteria were applied, including preferences for high resolution X-ray structures, gapless backbones, and high-sequence identity/similarity. Finally, the following templates were chosen to generate models of ALK: mouse c-Abl (1IEP, 1OPJ) and human INSR mutant (1IRK) for the closed conformation; mouse c-Abl (1M52) for the intermediate conformation; and human INSR and human LCK (1IR3, 3LCK) for the open conformation. ALK shares 34% identity and 48% similarity with Abl, 40% identity and 56% similarity with INSR, and 40% identity and 55% similarity with LCK in the kinase domain. Reliable pairwise sequence-structure alignments, needed for an accurate homology model, were obtained using the Verta algorithm of the Superimposer plugin of the program Bodil.[41] These pairwise alignments were merged to multiple alignments by the program malign,[42] using the STRMAT110 substitution matrix.[43] The homology modeling was performed with the program Modeller6v2,[44] using default parameters, including a round of minimization. For each conformation, 100 models were generated and their overall geometrical quality was accessed by Procheck.[45] The models showing geometrical qualities comparable to the templates were chosen for the docking studies. Furthermore a L1196T mutant of ALK corresponding to the NPM/ALK-L256T mutant was generated from all ALK models by using SYBYL 7.0 (Tripos, Inc., 1699 South Hanley Rd., St. Louis, Missouri, 63144, U.S.A.). The mutated protein was subjected to an energy minimization of 4 Å around the mutation to release possible strains introduced by altering L256.

Docking of PD17955, Imatinib, and SKI-606 in the ALK WT and L256T Homology Models. All dockings were performed using the program FlexX.[32] The docking protocol was validated by reproducing the binding mode of PD173955 in the A-chain of the Abl crystal structure of PDB entry 1M52 and the binding mode of imatinib in the Abl crystal structure of PDB entry 1IEP. The ligands were extracted from the crystal structure, charged using Gasteiger charges, and minimized with a convergence criterion of the gradient being 0.0001 to avoid the bias of a ligand conformation already having the optimal geometry to fit into the active site. The active site of the ALK models was defined by superimposing them onto the crystal structure of PDB entry 1IEP and taking into account all residues of the ALK model corresponding to the amino acids of Abl positioned 6.5 Å around imatinib of 1IEP. Thirty docking solutions were generated per docking run with FlexX.

Acknowledgment. We thank Pfizer (Groton, CT) for providing PD173955, Wyeth Research (Pearl River, NY) for SKI-606, Norvatis, Inc. (Basel, Switzerland), for imatinib, Dr. K. Pulford (John Radcliffe Hospital, Oxford, U.K.) for the anti-ALK1 antibody, Dr. P. G. Pelicci (European Institute of Oncology, Milan) for the NPM/ALK vector, and Mr. E. Marchesi (Istituto Nazionale dei Tumori, Milan, Italy) for technical assistance. This work was supported by the Italian Association for Cancer Research (AIRC), Min. San. Ricerca Finalizzata (2003), CNR, MIUR-COFIN and PRIN programs (2004), EU (Prokinase network, No. 503467), CFI, and NCI-C.

Supporting Information Available: Binding mode of imatinib in the active ALK-WT model. This material is available free of charge via the Internet at http://pubs.acs.org.

References

(1) Morris, S. W.; Naeve, C.; Mathew, P.; James, P. L.; Kirstein, M. N.; Cui, X.; Witte, D. P. ALK, the chromosome 2 gene locus altered by the t(2;5) in non-Hodgkin's lymphoma, encodes a novel neural receptor tyrosine kinase that is highly related to leukocyte tyrosine kinase (LTK). *Oncogene* **1997**, *14*, 2175−2188.

(2) Iwahara, T.; Fujimoto, J.; Wen, D.; Cupples, R.; Bucay, N.; Arakawa, T.; Mori, S.; Ratzkin, B.; Yamamoto, T. Molecular characterization of ALK, a receptor tyrosine kinase expressed specifically in the nervous system. *Oncogene* **1997**, *14*, 439−449.

(3) Morris, S. W.; Kirstein, M. N.; Valentine, M. B.; Dittmer, K. G.; Shapiro, D. N.; Saltman, D. L.; Look, A. T. Fusion of a kinase gene, ALK, to a nucleolar protein gene, NPM, in non- Hodgkin's lymphoma. *Science* **1994**, *263*, 1281−1284.

(4) Cook, J. R.; Dehner, L. P.; Collins, M. H.; Ma, Z.; Morris, S. W.; Coffin, C. M.; Hill, D. A. Anaplastic lymphoma kinase (ALK) expression in the inflammatory myofibroblastic tumor: a comparative immunohistochemical study. *Am. J. Surg. Pathol.* **2001**, *25*, 1364−1371.

(5) Gascoyne, R. D.; Lamant, L.; Martin-Subero, J. I.; Lestou, V. S.; Harris, N. L.; Muller-Hermelink, H. K.; Seymour, J. F.; Campbell, L. J.; Horsman, D. E.; Auvigne, I.; Espinos, E.; Siebert, R.; Delsol, G. ALK-positive diffuse large B-cell lymphoma is associated with Clathrin-ALK rearrangements: report of 6 cases. *Blood* **2003**, *102*, 2568−2573.

(6) Bai, R. Y.; Dieter, P.; Peschel, C.; Morris, S. W.; Duyster, J. Nucleophosmin-anaplastic lymphoma kinase of large-cell anaplastic lymphoma is a constitutively active tyrosine kinase that utilizes phospholipase C-gamma to mediate its mitogenicity. *Mol. Cell. Biol.* **1998**, *18*, 6951−6961.

(7) Slupianek, A.; Nieborowska-Skorska, M.; Hoser, G.; Morrione, A.; Majewski, M.; Xue, L.; Morris, S. W.; Wasik, M. A.; Skorski, T. Role of phosphatidylinositol 3-kinase-Akt pathway in nucleophosmin/anaplastic lymphoma kinase-mediated lymphomagenesis. *Cancer Res.* **2001**, *61*, 2194−2199.

(8) Zamo, A.; Chiarle, R.; Piva, R.; Howes, J.; Fan, Y.; Chilosi, M.; Levy, D. E.; Inghirami, G. Anaplastic lymphoma kinase (ALK) activates Stat3 and protects hematopoietic cells from cell death. *Oncogene* **2002**, *21*, 1038−1047.

(9) Bischof, D.; Pulford, K.; Mason, D. Y.; Morris, S. W. Role of the nucleophosmin (NPM) portion of the non-Hodgkin's lymphoma-associated NPM-anaplastic lymphoma kinase fusion protein in oncogenesis. *Mol. Cell. Biol.* **1997**, *17*, 2312−2325.

(10) Piva, R.; Chiarle, R.; Manazza, A. D.; Taulli, R.; Simmons, W.; Ambrogio, C.; D'Escamard, V.; Pellegrino, E.; Ponzetto, C.; Palestro, G.; Inghirami, G. Ablation of oncogenic ALK is a viable therapeutic approach for anaplastic large-cell lymphomas. *Blood* **2006**, *107*, 689−697.

(11) Coluccia, A. M.; Gunby, R. H.; Tartari, C. J.; Scapozza, L.; Gambacorti-Passerini, C.; Passoni, L. Anaplastic lymphoma kinase and its signaling molecules as novel targets in lymphoma therapy. *Expert Opin. Ther. Targets* **2005**, *9*, 515−532.

(12) Deininger, M.; Buchdunger, E.; Druker, B. J. The development of imatinib as a therapeutic agent for chronic myeloid leukemia. *Blood* **2005**, *105*, 2640−2653.

(13) Blanke, C. D.; Corless, C. L. State-of-the art therapy for gastrointestinal stromal tumors. *Cancer Invest.* **2005**, *23*, 274−280.

(14) Jones, A. V.; Cross, N. C. Oncogenic derivatives of platelet-derived growth factor receptors. *Cell. Mol. Life Sci.* **2004**, *61*, 2912−2923.

(15) Schindler, T.; Bornmann, W.; Pellicena, P.; Miller, W. T.; Clarkson, B.; Kuriyan, J. Structural mechanism for STI-571 inhibition of abelson tyrosine kinase. *Science* **2000**, *289*, 1938−1942.

(16) Nagar, B.; Bornmann, W. G.; Pellicena, P.; Schindler, T.; Veach, D. R.; Miller, W. T.; Clarkson, B.; Kuriyan, J. Crystal structures of the kinase domain of c-Abl in complex with the small molecule inhibitors PD173955 and imatinib (STI-571). *Cancer Res.* **2002**, *62*, 4236−4243.

(17) Fabbro, D.; Ruetz, S.; Buchdunger, E.; Cowan-Jacob, S. W.; Fendrich, G.; Liebetanz, J.; Mestan, J.; O'Reilly, T.; Traxler, P.; Chaudhuri, B.; Fretz, H.; Zimmermann, J.; Meyer, T.; Caravatti, G.; Furet, P.; Manley, P. W. Protein kinases as targets for anticancer agents: from inhibitors to useful drugs. *Pharmacol. Ther.* **2002**, *93*, 79−98.

(18) Eyers, P. A.; Craxton, M.; Morrice, N.; Cohen, P.; Goedert, M. Conversion of SB 203580-insensitive MAP kinase family members to drug-sensitive forms by a single amino acid substitution. *Chem. Biol.* **1998**, *5*, 321−328.

(19) Blencke, S.; Ullrich, A.; Daub, H. Mutation of threonine 766 in the epidermal growth factor receptor reveals a hotspot for resistance formation against selective tyrosine kinase inhibitors. *J. Biol. Chem.* **2003**, *278*, 15435−15440.

(20) Blencke, S.; Zech, B.; Engkvist, O.; Greff, Z.; Orfi, L.; Horvath, Z.; Keri, G.; Ullrich, A.; Daub, H. Characterization of a conserved structural determinant controlling protein kinase sensitivity to selective inhibitors. *Chem. Biol.* **2004**, *11*, 691−701.
(21) Bohmer, F. D.; Karagyozov, L.; Uecker, A.; Serve, H.; Botzki, A.; Mahboobi, S.; Dove, S. A single amino acid exchange inverts susceptibility of related receptor tyrosine kinases for the ATP site inhibitor STI-571. *J. Biol. Chem.* **2003**, *278*, 5148−5155.
(22) Gorre, M. E.; Mohammed, M.; Ellwood, K.; Hsu, N.; Paquette, R.; Rao, P. N.; Sawyers, C. L. Clinical resistance to STI-571 cancer therapy caused by BCR-ABL gene mutation or amplification. *Science* **2001**, *293*, 876−880.
(23) Cavalli, A.; Dezi, C.; Folkers, G.; Scapozza, L.; Recanatini, M. Three-dimensional model of the cyclin-dependent kinase 1 (CDK1): Ab initio active site parameters for molecular dynamics studies of CDKS. *Proteins* **2001**, *45*, 478−485.
(24) Thaimattam, R.; Daga, P. R.; Banerjee, R.; Iqbal, J. 3D-QSAR studies on c-Src kinase inhibitors and docking analyses of a potent dual kinase inhibitor of c-Src and c-Abl kinases. *Bioorg. Med. Chem.* **2005**, *13*, 4704−4712.
(25) von Bubnoff, N.; Veach, D. R.; Miller, W. T.; Li, W.; Sanger, J.; Peschel, C.; Bornmann, W. G.; Clarkson, B.; Duyster, J. Inhibition of wild-type and mutant Bcr-Abl by pyrido-pyrimidine-type small molecule kinase inhibitors. *Cancer Res.* **2003**, *63*, 6395−6404.
(26) Golas, J. M.; Arndt, K.; Etienne, C.; Lucas, J.; Nardin, D.; Gibbons, J.; Frost, P.; Ye, F.; Boschelli, D. H.; Boschelli, F. SKI-606, a 4-anilino-3-quinolinecarbonitrile dual inhibitor of Src and Abl kinases, is a potent antiproliferative agent against chronic myelogenous leukemia cells in culture and causes regression of K562 xenografts in nude mice. *Cancer Res.* **2003**, *63*, 375−381.
(27) Wisniewski, D.; Lambek, C. L.; Liu, C.; Strife, A.; Veach, D. R.; Nagar, B.; Young, M. A.; Schindler, T.; Bornmann, W. G.; Bertino, J. R.; Kuriyan, J.; Clarkson, B. Characterization of potent inhibitors of the Bcr-Abl and the c-kit receptor tyrosine kinases. *Cancer Res.* **2002**, *62*, 4244−4255.
(28) Burgess, M. R.; Skaggs, B. J.; Shah, N. P.; Lee, F. Y.; Sawyers, C. L. Comparative analysis of two clinically active BCR-ABL kinase inhibitors reveals the role of conformation-specific binding in resistance. *Proc. Natl. Acad. Sci. U.S.A.* **2005**, *102*, 3395−3400.
(29) Hubbard, S. R.; Wei, L.; Ellis, L.; Hendrickson, W. A. Crystal structure of the tyrosine kinase domain of the human insulin receptor. *Nature* **1994**, *372*, 746−754.
(30) Hubbard, S. R. Crystal structure of the activated insulin receptor tyrosine kinase in complex with peptide substrate and ATP analogue. *EMBO J.* **1997**, *16*, 5572−5581.
(31) Yamaguchi, H.; Hendrickson, W. A. Structural basis for activation of human lymphocyte kinase Lck upon tyrosine phosphorylation. *Nature* **1996**, *384*, 484−489.
(32) Rarey, M.; Kramer, B.; Lengauer, T.; Klebe, G. A fast flexible docking method using an incremental construction algorithm. *J. Mol. Biol.* **1996**, *261*, 470−489.
(33) Atwell, S.; Adams, J. M.; Badger, J.; Buchanan, M. D.; Feil, I. K.; Froning, K. J.; Gao, X.; Hendle, J.; Keegan, K.; Leon, B. C.; Muller-Dieckmann, H. J.; Nienaber, V. L.; Noland, B. W.; Post, K.; Rajashankar, K. R.; Ramos, A.; Russell, M.; Burley, S. K.; Buchanan, S. G. A novel mode of Gleevec binding is revealed by the structure of spleen tyrosine kinase. *J. Biol. Chem.* **2004**, *279*, 55827−55832.
(34) Wan, W.; Albom, M. S.; Lu, L.; Quail, M. R.; Becknell, N. C.; Weinberg, L. R.; Reddy, D. R.; Holskin, B. P.; Angeles, T. S.; Underiner, T. L.; Meyer, S. L.; Hudkins, R. L.; Dorsey, B. D.; Ator, M. A.; Ruggeri, B. A.; Cheng, M. Anaplastic lymphoma kinase activity is essential for the proliferation and survival of anaplastic large-cell lymphoma cells. *Blood* **2006**, *107*, 1617−1623.
(35) Li, R.; Xue, L.; Zhu, T.; Jiang, Q.; Cui, X.; Yan, Z.; McGee, D.; Wang, J.; Gantla, V. R.; Pickens, J. C.; McGrath, D.; Chucholowski, A.; Morris, S. W.; Webb, T. R. Design and synthesis of 5-aryl-pyridone-carboxamides as inhibitors of anaplastic lymphoma kinase. *J. Med. Chem.* **2006**, *49*, 1006−1015.
(36) Marzec, M.; Kasprzycka, M.; Ptasznik, A.; Wlodarski, P.; Zhang, Q.; Odum, N.; Wasik, M. A. Inhibition of ALK enzymatic activity in T-cell lymphoma cells induces apoptosis and suppresses proliferation and STAT3 phosphorylation independently of Jak3. *Lab. Invest.* **2005**, *85*, 1544−1554.
(37) Boschelli, D. H.; Ye, F.; Wang, Y. D.; Dutia, M.; Johnson, S. L.; Wu, B.; Miller, K.; Powell, D. W.; Yaczko, D.; Young, M.; Tischler, M.; Arndt, K.; Discafani, C.; Etienne, C.; Gibbons, J.; Grod, J.; Lucas, J.; Weber, J. M.; Boschelli, F. Optimization of 4-phenylamino-3-quinolinecarbonitriles as potent inhibitors of Src kinase activity. *J. Med. Chem.* **2001**, *44*, 3965−3977.
(38) Gunby, R. H.; Cazzaniga, G.; Tassi, E.; Le Coutre, P.; Pogliani, E.; Specchia, G.; Biondi, A.; Gambacorti-Passerini, C. Sensitivity to imatinib but low frequency of the TEL/PDGFRbeta fusion protein in chronic myelomonocytic leukemia. *Haematologica* **2003**, *88*, 408−415.
(39) Bairoch, A.; Boeckmann, B.; Ferro, S.; Gasteiger, E. Swiss-Prot: juggling between evolution and stability. *Briefings Bioinf.* **2004**, *5*, 39−55.
(40) Altschul, S. F.; Madden, T. L.; Schaffer, A. A.; Zhang, J.; Zhang, Z.; Miller, W.; Lipman, D. J. Gapped BLAST and PSI−BLAST: a new generation of protein database search programs. *Nucleic Acids Res.* **1997**, *25*, 3389−3402.
(41) Lehtonen, J. V.; Still, D. J.; Rantanen, V. V.; Ekholm, J.; Bjorklund, D.; Iftikhar, Z.; Huhtala, M.; Repo, S.; Jussila, A.; Jaakkola, J.; Pentikainen, O.; Nyronen, T.; Salminen, T.; Gyllenberg, M.; Johnson, M. S. BODIL: a molecular modeling environment for structure−function analysis and drug design. *J. Comput.-Aided Mol. Des.* **2004**, *18*, 401−419.
(42) Schneider, T. D.; Mastronarde, D. Fast multiple alignment of ungapped DNA sequences using information theory and a relaxation method. *Discrete Applied Mathematics* **1996**, *71*, 259−268.
(43) Johnson, M. S.; Overington, J. P. A structural basis for sequence comparisons. An evaluation of scoring methodologies. *J. Mol. Biol.* **1993**, *233*, 716−738.
(44) Marti-Renom, M. A.; Stuart, A. C.; Fiser, A.; Sanchez, R.; Melo, F.; Sali, A. Comparative protein structure modeling of genes and genomes. *Annu. Rev. Biophys. Biomol. Struct.* **2000**, *29*, 291−325.
(45) Laskowski, R. A.; MacArthur, M. W.; Moss, D. S.; Thornton, J. M. PROCHECK: a program to check the stereochemical quality of protein structures. *J. Appl. Crystallogr.* **1993**, *26*, 283−291.
(46) Beitz, E. TEXshade: shading and labeling of multiple sequence alignments using LATEX2 epsilon. *Bioinformatics* **2000**, *16*, 135−139.

JM060380K